Structural Studies on Hgr3 Orphan Receptor Ligand Prolactin-Releasing Peptide

Anna Maria D'Ursi,[†] Stefania Albrizio,[‡] Armida Di Fenza,[†] Orlando Crescenzi,[§] Alfonso Carotenuto,[†] Delia Picone,[§] Ettore Novellino,[‡] and Paolo Rovero*[,†]

Dipartimento di Scienze Farmaceutiche, Università di Salerno, Via Ponte Don Melillo 11C, I-84084 Fisciano, Salerno, Italy, Dipartimento di Chimica Farmaceutica e Tossicologica, Università degli Studi di Napoli Federico II, Via Montesano 49, I-80131 Napoli, Italy, and Dipartimento di Chimica, Università degli Studi di Napoli Federico II, Via Cintia, Complesso Universitario di Monte S. Angelo, I-80126 Napoli, Italy

Received June 25, 2002

Prolactin-releasing peptides (PrRPs) are two novel bioactive peptides of 20 and 31 residues, dubbed respectively PrRP20 and PrRP31, isolated from bovine hypothalamic tissues as ligands of the orphan seven-transmembrane domain receptor Hgr3. The first biological activity identified for these peptides was the release of prolactin. Recent data on biological activities of PrRPs as well as on the localization of their receptors in numerous central nervous system sites suggested new potential actions of PrRPs in the regulation of the central nervous system and the possibility of identifying an alternative central role for these peptides. We describe here the synthesis and the structural characterization of the peptide PrRP20 by CD and NMR spectroscopies. A 3D model was built on the basis of the NMR data collected in a water/sodium dodecyl sulfate mixture. This system provides an amphipatic medium able to mimic the cell membrane. The main structural feature of the PrRP20 is an α-helical secondary structure spanning the 10 C-terminal residues. The conformational properties of PrRP20 are discussed in considering the sequence similarity observed between the Hgr3 and the neuropeptide Y (NPY) receptors. This similarity, together with the data showing a number of biological activities common to PrRP and NPY peptides, leads us to formulate the hypothesis that similar structural elements could exist in the ligands as well. In fact, PrRP20 and NPY are well aligned in the C-terminal portion, where they share an amphipatic α-helical secondary structure. Interestingly, the homology between the two sequences involves residues crucial for NPY biological activity. The conformational characterization of PrRP20 and the comparison with NPY are a valuable starting point for the rational design of subsequent SAR studies aimed at identifying PrRP analogues acting as either agonists or antagonists at the Hgr3 receptor. Such PrRP analogues could be useful receptorial tools able to clarify the multiple biological functions hypothesized for the PrRP receptor in the central nervous system.

Introduction

Recent advances in DNA sequencing technologies have led to the acquisition of a great deal of information about the human genome. Such information has an enormous potential to be exploited to identify a wide range of new molecular targets of pharmaceutical interest. Particularly promising in this context is the newly defined family of the so-called "orphan receptors", which are G-protein-coupled receptors identified through genomic studies, whose ligands remain to be identified.[1,2]

G-protein-coupled receptors are a superfamily of transmembrane receptors involved in numerous different signaling pathways. They are responsive to different agents such as hormones, neurotransmitters, and chemokines and play an important role in sensory perception, including vision and smell.[3] Their participation in a broad range of physiological processes has made them excellent drug targets. Within the past 20 years, a large number of new drugs acting as agonist or antagonist for GPCRs have been registered.[1,2] Consistently, the discovery of new GPCR types and the characterization of their ligands represent an opportunity to discover new drugs. In particular, a new pharmacological strategy called "reverse pharmacology" aimed at characterizing orphan receptor and discovering the respective ligands[4] has been widely exploited recently. This approach starts with an orphan receptor of unknown function, which is used as a "hook" to fish out the ligand. The use of the ligand to explore the biological and pathophysiological role of the receptor is the second and important step of the reverse pharmacology approach.

A notable example of peptides recently identified as ligands of an orphan receptor is represented by the prolactin releasing peptides (PrRPs), two related sequences of 20 (PrRP20) and 31 (PrRP31) amino acids derived from a common precursor:[5,6]

PrRP20 TPDINPAWYASRGIRPVGRF

PrRP31 SRTHRHSMEIRTPDINPAWYASRGIRPVGRF

They were initially identified as ligands of an orphan

* To whom correspondence should be addressed. Phone: 0039089962809. Fax: 0039089962828. E-mail: rovero@unisa.it.
[†] Università di Salerno.
[‡] Dipartimento di Chimica Farmaceutica e Tossicologica, Università degli Studi di Napoli Federico II.
[§] Dipartimento di Chimica, Università degli Studi di Napoli Federico II.

10.1021/jm020975p CCC: $22.00
Published on Web 11/07/2002

receptor known as GPR10[7,8] and then renamed Hgr3.[1,2] The first biological function identified for the PrRP peptides was the prolactin release from pituitary cells,[5,6] mediated by receptors localized in the anterior pituitary. More recent reports have questioned the central role of PrRP in neuroendocrine control of lactotroph function. The identification of PrRP receptors and PrRP mRNA in numerous CNS sites[9,10] has suggested a new potential action of PrRP in the regulation of the CNS, disclosing the possibility identifying an alternative central role for these peptides. Some recent studies have demonstrated effects of the PrRP peptides on the secretion of various hypothalamic hormones such as corticotropin-releasing hormone[11] and luteinizing hormone/follicle-stimulating hormone,[12] as well as on food intake.[13,14] Furthermore, it has been recently demonstrated that the Hgr3 receptor may modulate neurotransmission specifically at glutamatergic synapses through the interaction with the same PDZ domain proteins[15] that interact with AMPA receptors.

Like the majority of orphan receptors, Hgr3 shows a low level of sequence homology with known GPCRs. Notwithstanding, a certain degree of match has been reported to members of the neuropeptide Y (NPY) family of receptors.[2] The similarity of the NPY and Hgr3 receptor sequences prompted us to investigate the hypothesis that a similarity in the structure of the ligands could exist as well. Neuropeptide Y is a 36-residue C-terminally amidated polypeptide hormone and neurotransmitter.[16] It is widely expressed in the CNS as well as in the peripheral nervous system. NPY has been implicated in various physiological responses including cardiovascular regulation and the control of food intake.[16,17] The molecular conformation of NPY has been discussed in the literature both extensively and controversially. All the data converge with the presence of an α-helix involving the 20 C-terminal residues, whereas the N-terminus part seems more flexible and is influenced by the medium environment.[18−21] Recently the structure and dynamics of micelle-bound NPY have been reported and the hypothesis of a decisive role played by the membrane association on receptor binding of this peptide has been proposed.[22] These new findings are very interesting and will be discussed in the present paper in view of the hypothesized structural similarity between NPY and PrRPs.

PrRPs are relatively unknown peptides. The biological activities and the receptor localization are still under investigation.[7−15] Most notably, neither the structure−activity relationship nor the structural propensity of these peptides has been reported in the literature to date. We describe here a conformational analysis of PrRP20 performed by means of CD, 2D NMR, and molecular modeling calculations. On the basis of the reported receptor sequences similarity, we analyzed the PrRP20 structural data in comparison with the literature data available for the neuropeptide Y. CD and NMR spectra were recorded in different medium environments, including SDS solution. To compare our data with a recently published micelle-bound structure of NPY,[22] the building of a 3D model was made starting from NMR data obtained in the latter medium. Furthermore, to have data on the orientation of the PrRP peptide relative to the micelle compartments, we performed a series of NMR experiments in the presence of spin-label compounds.

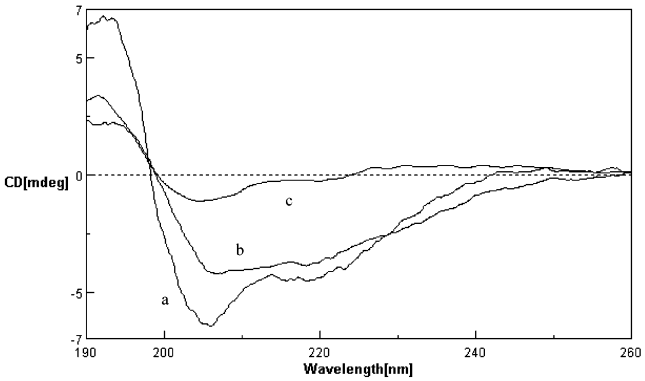

Figure 1. Circular dichroism spectra of PrRP20, recorded at room temperature in 100 mM water solution of SDS (a), in water/HFA solution, 50/50 v/v (b), and in water (c).

The structural characterization of the PrRP20 peptide is a valuable starting point for the rational design of subsequent SAR studies aimed at identifying PrRP analogues acting as agonists or, most importantly, antagonists at the Hgr3 receptor. At this stage, such PrRP analogues would be useful receptorial tools able to shade light on the multiple biological functions proposed for the PrRP receptor in the CNS.

Results and Discussion

Circular Dichroism. The conformational behavior of PrRP20 in solution was investigated by means of circular dichroism. The CD spectra of PrRP20 were recorded in water, in HFA/water 50/50 v/v, and in SDS/water mixtures (Figure 1). The exploration of other solvent mixtures was hampered by the low solubility properties of the peptide. The CD spectra of PrRP20 in water lack any of the features typical of secondary structure. The secondary structure analysis of the CD data in HFA/water suggests the presence of disordered conformers with comparable amounts of random coil, turn, and β-structures.

It is well-known that water is the best medium to be used for the structural study of peptides. Unfortunately it favors the prevailing of disordered and flexible conformations so that the building of a 3D model is precluded. An exploration of different solvents is necessary in order to set solution conditions able to limit the conformational freedom. At the same time, the biocompatibility of the medium is essential to having biological reliability of the results. Mixtures made up of water and organic solvents are the most used media to produce environmental constraints. Their biocompatibility has been shown.[23−25] In particular, alcohols and fluoro alcohols are known to induce helicity in peptides.[26−28] Recently HFA/water mixtures have been proposed because they behave like TFE/water mixtures but with a much higher helix-inducing propensity.[29] The conformational behavior of the PrRP20 in water/HFA solutions demonstrates that the helix-inducing propensity of HFA does not override the intrinsic tendency of the peptide. It defines a paradigmatic case similar to that reported for β-endorphin,[30] showing that even in a strong helix-inducing solvent the coexistence of helical conformations, turns, and disordered stretches can be

Table 1. ^{1}H Chemical Shift Assignments for PrRP20 in 100 mM SDS at 600 MHz and 300 K[a]

residue	Δ in chemical shift	NH	CH_α	CH_β	CH_γ	CH_δ	others
Thr[1]	−0.16	7.68	4.19	4.11	CH_3 1.34		
Pro[2]	0.06		4.50	2.33 1.99	1.94 1.79	3.85 3.57	
Asp[3]	−0.03	8.40	4.73	2.93 2.78			
Ile[4]	−0.20	7.79	4.03	1.81	1.36 1.06		
				γCH_3 0.81	δCH_3 0.72		
Asn[5]	−0.43	7.89	4.32	2.80 2.78			γNH_2 7.48 6.78
Pro[6]	−0.29		4.15	1.74 1.76	1.59 1.61	3.29 3.11	
Ala[7]	−0.14	8.17	4.21	CH_3 1.34			
Trp[8]	−0.36	7.79	4.34	3.29 3.02			2H 7.21 4H 7.39
							5H 6.98 6H 7.06
							7H 7.40 NH 9.93
Tyr[9]	−0.57	7.49	4.03	2.87 2.78			2,6H 6.93
							3,5H 6.76
Ala[10]	−0.21	7.86	4.14	CH_3 1.38			
Ser[11]	−0.19	7.79	4.31	3.90 3.85			
Arg[12]	−0.20	7.66	4.18	1.77 1.65	1.51 1.49	2.89 2.91	H_ϵ 6.98
Gly[13]	−0.12	8.04	3.86 3.84				
Ile[14]	−0.11	7.60	4.12	1.82	1.44 1.13		
				γCH_3 0.89	δCH_3 0.84		
Arg[15]	0.27	7.96	4.65	1.86 1.77	1.63 1.61	3.19 3.17	H_ϵ 7.11
Pro[16]	−0.04		4.46	2.27 2.03	1.98 1.96	3.72 3.74	
Val[17]	−0.04	7.84	4.14	2.18			
				CH_3 0.96 0.94			
Gly[18]	−0.04	8.19	3.94 3.92				
Arg[19]	−0.33	7.93	4.05	1.57 1.44	1.11 0.97	2.94 2.92	H_ϵ 6.94
							NH 7.24
Phe[20]	−0.06	7.92	4.60	3.27 2.95			2,6H 7.33
							3,5H 7.24
							6H 7.13

[a] All values are referenced to the water residue signal.

observed, depending on the intrinsic tendency of the amino acid sequence.

In aqueous SDS solution (100 mM), the shape of the CD spectrum suggests the presence of α-helical folding with two minima at 208 and 222 nm and a maximum at 198 nm. The use of SDS micelles to study the conformational properties of PrRP20 is motivated on the basis of its interaction with a membrane receptor. For peptides acting as ligands of membrane receptors, the use of membrane mimetic media such as SDS and dodecylphosphocoline is suggested, hypothesizing a membrane-assisted mechanism of interactions between the peptides and their receptors.[31,32] According to this model, the membrane surface plays a key role in facilitating the transition of the peptide from a random coil conformation adopted in the extracellular environment to a conformation that is recognized by the receptor.[33,34] The increase of the local concentration of the peptide and the reduction of the rotational and translational freedom of the neuropeptide are membrane-mediated events acting as determinant steps for the conformational transition of the peptide.[35−37]

NMR Spectrometry. A whole set of 1D and 2D protonic spectra were recorded in a 100 mM aqueous solution of SDS. To check the absence of an aggregation state of the peptide, spectra were acquired in the concentration range 0.5−15 mM. No significant changes were observed in the distribution and in the shape of the ^{1}H resonances, indicating that no aggregation phenomena occurred in this concentration range. Complete assignments of the proton spectra of PrRP20 were achieved according to the Wuthrich procedure[38] via the usual systematic application of DQF-COSY, TOCSY, and NOESY experiments[39−41] with the support of the XEASY software package.[42] Table 1 reports the proton chemical shift assignment of PrRP20 in SDS micelles solution. CH_α resonances are strongly dependent on local secondary structure.[43,44] Upfield shifts, relative to random coil values, are generally found for residues implicated in an α-helix or in turns and downfield shifts for those in β-sheets. Consistent with the CD data on the existence of turn and helical conformation, the CH_α proton of the PrRP20 experiences an upfield shift of the NMR signals with respect to those observed for the same amino acids in the random coil state (Table 1).

In Figure 2, the downfield region of the NOESY spectrum recorded in a mixture of water/SDS is shown. Cis−trans isomerism around the $Xaa_{i-1}-Pro_i$ bonds was investigated at the level of the Pro residues present in positions 2, 6, and 16 of the PrRP20 sequence. The presence of NOE contacts between $H_{2\delta}$Pro and the amide proton of the preceding residue in the sequence for all three Pro residues showed that the prevalent conformers are characterized by an $Xaa_{i-1}-Pro_i$ trans conformation. The presence of small signals close to the cross-peaks that define the patterns of the Pro indicates the presence of a minor but observable population of cis isomers.

All short- and medium-range NOE effects involving the backbone protons of PrRP20 in a water/SDS mixture are summarized in Figure 3. The whole sequence is characterized by a series of sequential NH_i-NH_{i+1} NOEs, consistent with a nascent helical structure,[45] and diagnostically critical (i, $i + 2$) and (i, $i + 3$) effects typical of a regular helix can be observed for the entire stretch of residues 11−19. The N-terminal region of the peptide lacks a regular NOE pattern, thus suggesting a prevalence of disordered structures and notwithstanding the presence of diagnostic $CH_{\alpha i}-CH_{2\beta i+3}$ and NH_i-NH_{i+1} indicating a weak tendency to form a turn structure around the Pro[2] residue.

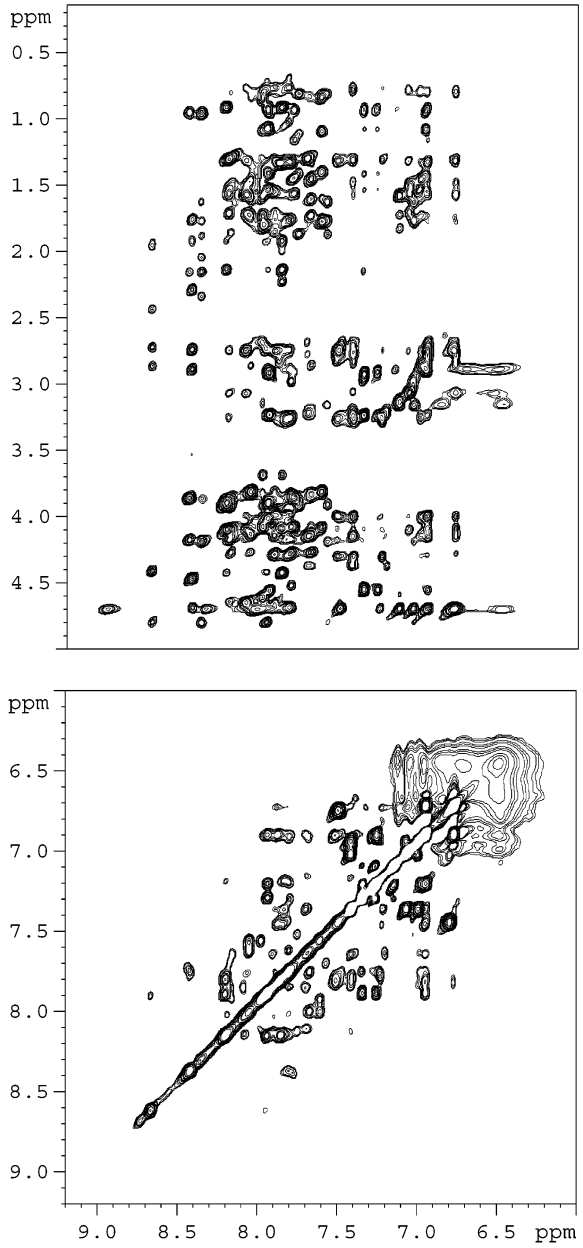

Figure 2. Fingerprint region (bottom) and amide region (top) of the NOESY spectra of PrRP20 in 100 mM SDS/water solution (600 MHz, $T = 300$ K, 1.8 mM).

Structure Calculation. NMR data in SDS/water solution were the starting point for the building of a 3D model. Three-dimensional structures were calculated by simulated annealing in torsion angle space and restrained molecular dynamics methods based on NOE-derived restraints, using the DYANA software package.[46] Among 50 calculated structures, the resulting 20 best ones were selected according to the lowest values of their target function. They were subjected to further procedures of minimization with the SANDER module of AMBER 5.0 software[47,48] using the DYANA derived restraints.

Consistent with the NOE patterns reported in Figure 3, the NMR calculated models show the presence of significantly regular structures in the C-terminal region. Figure 4 shows the superposition of the backbone heavy atoms of residues 11−19 of the 20 best calculated structures (heavy atoms backbone rmsd is 0.85). For

Figure 3. Summary of sequential and medium-range NOEs for PrRP20. Data were obtained from 600 MHz NOESY experiments (mixing time of 200 ms) recorded in 100 mM SDS/water solution.

Figure 4. Twenty best calculated structures of PrRP20 (green) as derived from DYANA calculation and energy-minimized using the SANDER module of AMBER 5.0 software. The structures are fitted on the heavy backbone atoms of the 11−19 segment. The helical arrangement of residues 11−19 is highlighted by a yellow tube ribbon.

residues 11−19, the pattern of dihedral angles in this region is typical of an α-helical arrangement. It is interesting to note, among the residues involved in the helical arrangement, the presence of small (Gly and Pro) and hydrophobic (Ile and Val) residues. These residues, according to the results of a study relative to the internal packing of helical membrane proteins,[49] define the typical composition of helices located inside or in proximity of a hydrophobic environment. In agreement with NOE data summarized in Figure 3, the N-terminal

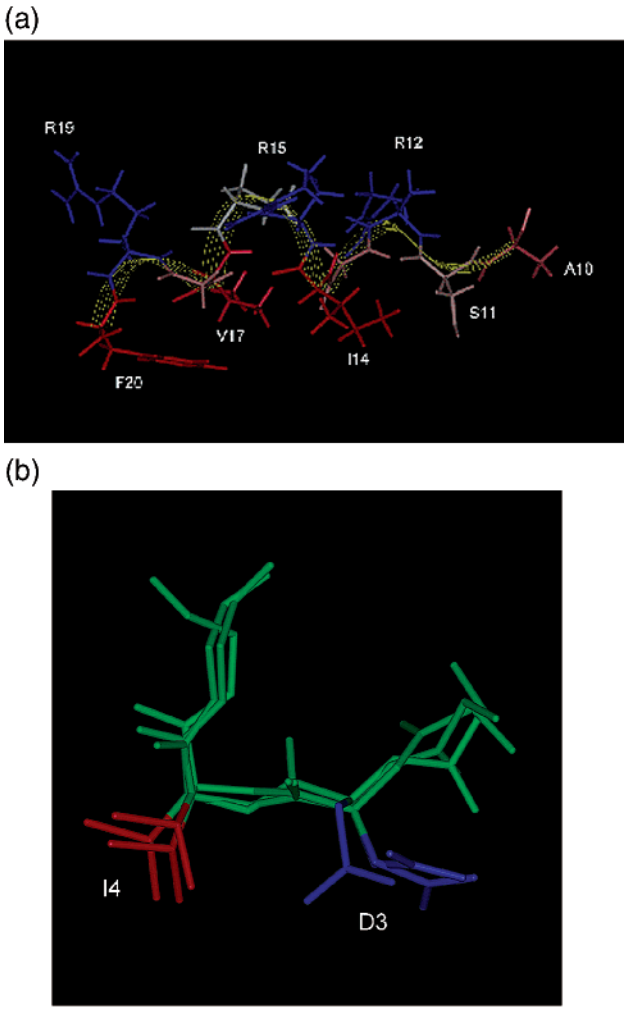

Figure 5. PrRP20 structures of residues 11−19 (a) and 1−6 (b). The structures were chosen according to the lowest value of the target function. Side chains are colored according to their hydrophobic character. High, medium, and low hydrophobic residues are colored, respectively, in red, gray/light-blue, and blue.

region is more flexible with a weak tendency to form a β-turn structure that includes residues 2−5.

Also interesting is the analysis of the side chain distribution. The C-terminal helical portions of PrRP20 NMR structures define an amphipatic system (Figure 5a) where one side of the helical surface is hydrophobic because of the presence of the apolar side chains of Ala[10], Ile[14], Val[17], and Phe[20] residues and where the other side is hydrophilic because of the polar side chains of Arg[12], Arg[17], and Arg[19] residues. On the other hand, the side chains of Asp[3] and Ile[4] belonging to the N-terminal turn structure of the peptide display a well-defined arrangement with a common preferred orientation (Figure 5b).

Spin-Label Studies. The positioning of the peptide relative to the surface and interior of the SDS micelle was studied using paramagnetic probes: 5-doxylstearic acid and 12-doxylstearic acid. All of these compounds contain doxyl headgroups, a cyclic nitroxide with an unpaired electron that is bound to the aliphatic chain carbon in position 12 or 5. Unpaired electrons lead to dramatically accelerated longitudinal and transverse relaxation rates of protons in spatial proximity via highly efficient spin and electron relaxation. Therefore, these paramagnetic probes are expected to cause broadening of the NMR signals and a decrease of resonance intensities from residues inside but close to the surface (5-doxyl) or deeply buried in the micelle (12-doxyl).[50,51]

TOCSY spectra of PrRP20 in the presence and in the absence of the spin labels, with all other conditions kept constant, were recorded. All signal intensities remained constant after addition of 12-doxylstearic acid, thereby proving that no residues of PrRP20 become embedded in the hydrophobic core of the micelle (data not shown). In the presence of 5-doxylstearic acid, the ratios of volumes of several NH/α signals from experiments performed in the presence of the spin label to those from a control sample without spin label were broadened and decreased in intensity. This provides evidence that PrRP20 is located at the liquid−water interface with its ordinate regions parallel to the membrane. In parts a and b of Figure 6, a comparison of the NH/α region of TOCSY spectra of PrRP20 acquired in the presence and in absence of 5-doxylstearic acid is reported. Asp[3], Ile[4], Trp[8], Tyr[9], Ile[14], Val[17], and Phe[20] are drastically affected by the spin-label effect with a near-disappearance of the NH/α signals. Ile[14], Val[17], and Phe[20] lining the surface of an amphipatic helix reasonably induced by the micellar environment leads us to hypothesize a similar orientation of the peptide in the cell membrane environment where the receptor is located. On the other hand, Ile3 and Asp4 as well as Trp8 and Tyr9 side chains are arranged with a well-defined orientation and we are able to locate the peptide on the surface of the membrane at the level of its more ordered structural stretches.

Sequence Analysis. As reported in the Introduction, the Hgr3 receptor shows a low level of sequence homology with known GPCRs. Notwithstanding, its closest match is to members of the NPY family of receptors.[2] The similarity of the receptor sequences has induced us to compare the structures of these two neuropeptides. Figure 7a shows the sequence alignment of NPY and PrRP31, obtained with the software ClustalW.[52] To improve the efficiency of the alignment, we used the longer PrRP sequence, i.e., that of PrRP31, whose length is more comparable to that of NPY. A comparison of the sequences shows that four identities, three strong homologies and one weak homology, are found among the 13 C-terminal residues. An analysis of these homologies in light of the known NPY structure−activity relationship data[53] indicates that the conserved and homologous residues (Figure 7a) are among the most important for NPY biological activity. In particular, PrRP Arg[19] corresponds to NPY Arg[35]; this residue has been reported to be crucial for NPY activity, since the single replacement of Arg[35] by Ala leads to a complete loss of affinity at all cloned NPY receptor subtypes.[53]

The C-terminal is amidated in both peptides, and this is again a key element in NPY activity, since it has been demonstrated that the negatively charged free carboxylic group at the C-terminus prevents this peptide from binding to all receptor subtypes. Interestingly, the C-terminal residues are highly homologous (NPY Tyr vs PrRP31 Phe). The importance of this homology is supported by the observation that upon substitution of

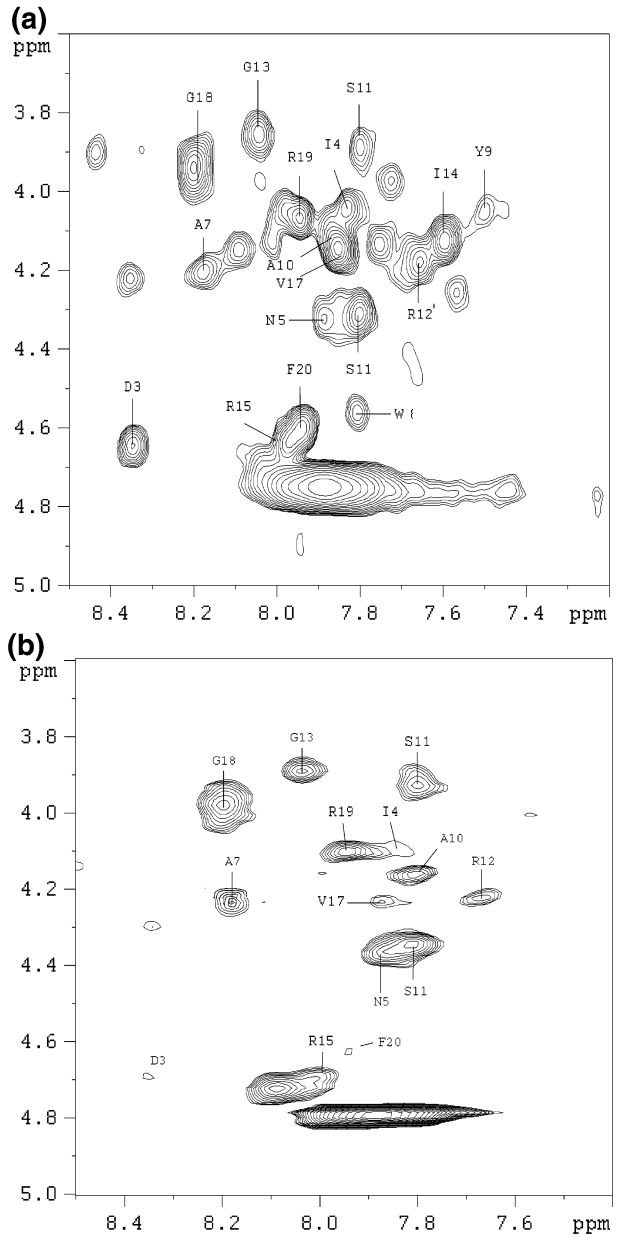

Figure 6. Amide region of the TOCSY spectra of PrRP20 in 100 mM SDS/water solution (600 MHz, $T = 300$ K, 1.8 mM). Panel a shows the fingerprint region of PrRP20 recorded in 100 mM SDS/water solution. Panel b shows the fingerprint region of PrRP20 with 5-doxylstearic acid at a concentration of one spin label per micelle added.

NPY C-terminal Tyr[36]-amide by Phe-amide the affinity remains in the nanomolar range.[53]

PrRP20 residues Ile[14], Val[17], and Phe[20] are well aligned with NPY Ile[28], Thr[32], and Tyr[36], respectively. In Figure 7b, a comparison of the PrRP20 NMR structure obtained in the present study with the published NPY micelle NMR structure[22] (PDB code 1F8P) is displayed. It is evident that the structures are characterized by a common structural arrangement in the region that includes the aligned residues. The helices of the two structures present a common distribution of the hydrophobic and hydrophilic side chains, defining both amphipatic systems. As reported in the quoted paper of Bader et al., with respect to the helical periodicity, the signal intensities of the residues Ile[28], Thr[32], and Tyr[36] are more affected by the spin label than by their neighboring residues. Interestingly the residues of PrRP20 corresponding in the sequence alignment to Ile[28], Thr[32], and Tyr[36] (i.e., Ile[14], Val[17], Phe[20], respectively) are characterized by the same property as being drastically sensitive to the 5-doxylstearic acid.

This result supports the hypothesis of a structural similarity between the PrRP20 and NPY where the two peptides seem to share a common orientation with respect to the cell membrane, mimicked in solution by the micelle environment. This observation is particularly relevant because the micelle-bound structure of NPY recently published supports, with a wealth of experimental data, the model originally theorized by Schwyzer.[33−37] According to this model, the target cell membrane influences receptor selection of regulatory peptides by leading important residues into the appropriate compartments. Thus, the α-helix itself, but also its particular orientation and amphiphilicity, may be required to provide the conformational prerequisites of residues important for the receptor binding. Consistently, Bader et al.[22] demonstrate that the NPY C-terminal amide serves as an anchor to the membrane, thereby stabilizing the helix at the C-terminus, restricting the conformational space, and possibly inducing the bioactive conformation. Similarly, the anchoring of NPY to the membrane via the Ile[31] residue may provide the proper positioning/preorientation of the residues implicated in the direct interaction with the receptor, thus facilitating receptor recognition. Generally speaking, the sequence alignment of PrRP31 and NPY, the comparison of their structures, and the common orientation with respect to the micelles lead us to hypothesize that a common procedure of preorientation and preparation of the receptor binding exists. In fact, the single residues responsible for the binding to the membrane, the overall backbone structure, and the orientation with respect to the membrane compartment are conserved. The residues that are significantly different between the two peptides in terms of both sequence and structure are those that in NPY account for the receptor subtype specificity. This observation suggests their possible role in being responsible for the peculiarity of the interactions of the PrRP peptides with their specific receptor(s).

It is clear that the speculations made on the similarity between PrRP and NPY need experimental demonstration. Nevertheless, this could be a valuable starting point for the design of PrRP analogues to be used as pharmacological tools, particularly useful since classical SAR data are still not available. In particular, recent studies provide evidence for PrRP neurons forming part of the leptin-sensitive brain circuitry involved in the regulation of food intake and energy homeostasis,[13,14] a field in which the search for new drug candidates is very active. Finally, the reported data assume further utility and importance in light of the visibility and the interest that the PrRP receptor has recently assumed as ligand of the PDZ domain.[15]

Experimental Section

Peptide Synthesis. The peptide was synthesized by the solid-phase method using a Milligen 9050 automatic synthesizer with Fmoc/tBu chemistry and continuous flow technology. The synthesis was performed using 0.4 g of TentaGel S AM resin (substitution level of 0.25 mmol/g) to obtain a C-terminal

(a)

```
PRRP_HUMAN     --SRTHRHSMEIRTPDINPAWYASRG-IRP-VG-RF 31
NEUY_HUMAN     YPSKPDNPGEDAPAEDMARYYSALRHYINLITRQRY 36
                 *:... . :  : *:   : * *  *. :   *:
```

(b)

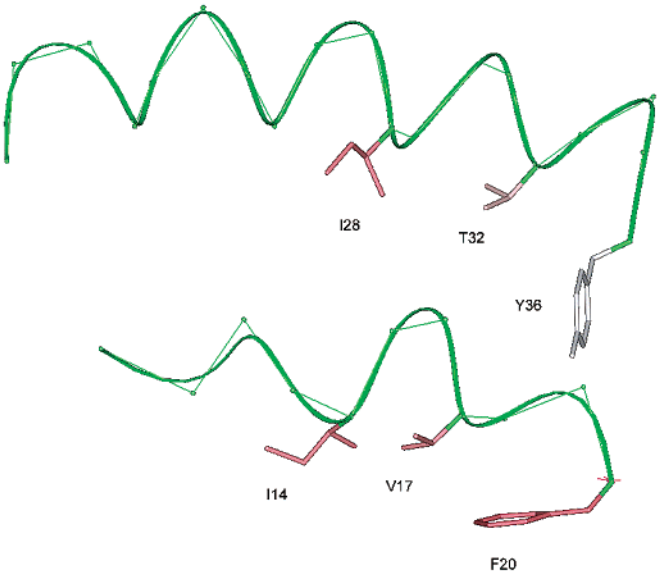

Figure 7. (a) Pairwaise alignment of PrRP31 and NPY sequence. The alignment was performed with ClustalW software. The asterisks indicate conserved residues. Single points indicate low homology between the paired residues, and double points indicate high homology between the paired residues. (b) Comparison of the 12−20 portion of the PrRP20 NMR structure chosen according to the lowest value of the target function, with the 16−36 region of the micelle NMR structure of neuropeptide Y (PDB code 1F8P). The secondary structures are highlighted by a green ribbon The side chains having a higher hydrophobicity are in red, and the side chains having a lower hydrophobicity are in gray.

amide by acidic cleavage (AM is 5-(4-aminomethyl-3,5-dimethoxyphenoxy)butanoic acid linker; TentaGel is polystyrene-supported polyoxyethylene scaffold). The following side chain protections were used: tBu for Asp, Thr, Tyr, and Ser; Trt for Asn; Pmc for Arg; Boc for Trp. The following synthetic cycles were used: Fmoc deprotection (20% piperidine in DMF, 5 min at 12 mL/min); DMF washing (12 min at 6 mL/min); coupling (4-fold excess of Fmoc-amino acid, HBTU, HOBt, and NMM in DMF, recycle 20 min at 12 mL/min); DMF washing (8 min at 6 mL/min). Cleavage from the resin and side chain deprotection were achieved by treatment of the dried peptide resin with 20 mL of a mixture of trifluoroacetic acid/thioanisole/ethanedithiol/water/phenol (82.5/5/2.5/5/5 v/v) for 100 min at room temperature. The crude peptide was precipitated with cold ether and lyophilized. The yield was 208 mg (89%, calculated on the resin loading). The crude peptide was analyzed by HPLC on a Beckman System Gold apparatus under the following conditions: Vydac C_{18} column (0.46 cm × 15 cm); eluant A, 0.1% TFA/water; eluant B, 0.1% TFA/acetonitrile; gradient from 5% to 65% eluant B over 20 min; flow of 1 mL/min; detection, UV, 210 nm; R_t = 12.2 min; HPLC purity, 64% (expressed as peak height %). The main peak was isolated by preparative HPLC, using a Vydac C_{18} column (2.2 cm × 25 cm). The conditions are the following: eluants A and B as indicated above; gradient from 15% to 44% eluant B over 120 min; flow of 4 mL/min; detection, UV, 210 nm. The final product (HPLC purity > 99%) was characterized by ES-MS, yielding the correct molecular mass of 2331.9 Da.

Circular Dichroism. All CD spectra were recorded using a JASCO J810 spectropolarimeter with a cell of 1 mm path length. The CD measurements were performed in the range from 260 to 190 nm with a 1 nm bandwidth, 4 accumulations, and 10 nm/min of scanning speed at room temperature. The pH of the aqueous sample was adjusted to 5.5 by adding a small amount of phosphate buffer solution. Peptide (0.1 mM) concentration was determined spectrophotometrically using tyrosine and tryptophan absorbance as described.[54] The SDS sample was obtained by dissolving the peptide in an aqueous solution of 100 mM SDS, pH 5.5. A solution of water/HFA, 50/50 v/v, were prepared. The concentration of the peptide in this solution was 0.1 mM. For estimation of secondary structure content, CD spectra were analyzed by a linear combination fit using the reference data of Greenfield and Fasman.[55]

NMR Spectrometry. The sample for NMR spectrometry was prepared by dissolving the appropriate amount of PrRP20 in 0.5 mL of an aqueous solution (pH 5.5) to obtain 1 mM of peptide and 100 mM of SDS-d_{25}. NMR spectra were recorded on a Bruker DRX-600 spectrometer. One-dimensional (1D) NMR spectra were recorded in the Fourier mode with quadrature detection, and the water signal was suppressed by low-power selective irradiation in the homogated mode. DQF-COSY, TOCSY, and NOESY[38−40] experiments were run in the phase-sensitive mode using quadrature detection in ω_1 by time-proportional phase increase of the initial pulse. Data block sizes were 2048 addresses in t_2 and 512 equidistant t_1 values. Before Fourier transformation, the time domain data matrices were multiplied by shifted $\sin^2$ functions in both dimensions. A mixing time of 70 ms was used for the TOCSY experiments. NOESY experiments were run at 300 K with mixing times in the range 100−250 ms. The qualitative and quantitative analyses of DQF-COSY, TOCSY, and NOESY spectra were achieved using the XEASY software.[41]

Spin-Label Experiments. The NMR samples were prepared by dissolving 2 mM PrRP20 in 100 mM deuterated SDS solution in H_2O/D_2O. Assuming an SDS micelle aggregation number of 56, this corresponds to a micelle concentration of 1.8 mM. The H_2O/D_2O ratio was 90/10.[56] The 5- and 12-doxylstearic acids were solubilized in methanol-d_4 and then added to the samples.

Molecular Modeling. Peak volumes were translated into upper distance bounds with the routine CALIBA of the DYANA software.[45] The necessary pseudoatom corrections were applied for nonstereospecifically assigned protons at prochiral centers and for the methyl group. After discarding

redundant and duplicated constraints, the final list included 51 intraresidue and 113 interresidue constraints, which were used to generate an ensemble of 100 structures by the standard protocol of simulated annealing in torsion angle space implemented in DYANA (using 6000 steps). No dihedral angle restraints and no hydrogen bond restraints were applied. The best 20 structures, which had low values of the target functions (0.83−1.19) and small residual violations (maximum violation of 0.38 Å), were refined by in vacuo minimization in the AMBER 1991 force field, using the program SANDER of the AMBER 5.0 suite.[46,47] To mimick the effect of solvent screening, all net charges were reduced to 20% of their real value and moreover a distance-dependent dielectric constant ($\epsilon = r$) was used. The cutoff for nonbonded interactions was 12 Å. The NMR-derived upper bounds were imposed as semiparabolic penalty functions with force constants of 16 kcal mol^{-1} $Å^{-2}$; the function was shifted to linear when the violation exceeded 0.5 Å. The 10 best structures after minimization had AMBER energies ranging from −441.4 to −391.1 kcal/mol. The final structures were analyzed using the Insight 98.0 program.[57] Computations were performed on SGI Indigo II computers.

Acknowledgment. This work was supported by grants from Ministero dell'Università e della Ricerca Scientifica e Tecnologica and Fondi di Ateneo Università degli Studi di Salerno.

Appendix

Abbreviations. Abbreviations used for amino acids and the designation of peptides follow the rules of the IUPAC-IUB Commission of Biochemical Nomenclature in *J. Biol. Chem.* **1972**, *247*, 977−983. Amino acid symbols denote L-configuration unless indicated otherwise. The following additional abbreviations are used: PrRP, prolactin-releasing peptide; SDS, sodium dodecyl sulfate; CNS, central nervous system; NPY, neuropeptide Y; SAR, structure−activity relationship; GPCR, G-protein-coupled receptors; NMR, nuclear magnetic resonance; CD, circular dichroism; Fmoc, fluorenylmethoxycarbonyl; HPLC, high-performance liquid chromatography; HFA, hexafluoroacetone trihydrate; DQF-COSY, double-quantum-filtered correlation spectroscopy; TOCSY, total correlation spectroscopy; NOESY, nuclear Overhauser effect spectrometry; NOE, nuclear Overhauser enhancement; MD, molecular dynamic; 1D, 2D and 3D, one-, two- and three-dimensional; PDZ, PSD, Disc-large-ZO-1; AMPA, α-amino-3-hydroxy-5-methylisoxazole-4-propionic acid.

References

(1) Stadel, J. M.; Wilson, S.; Bergsma, D. J. Orphan G-protein-coupled receptors, a neglected opportunity for pioneer drug discovery. *TIPS* **1997**, *18*, 430−437.

(2) Wilson, S.; Bergsma, D. J.; Chambers, J. K.; Muir, A. I.; Fantom, K. G. M.; Ellis, C.; Murdock, P. R.; Herrity, N. C.; Stadel, J. M. Orphan G-protein-coupled receptors, the next generation of drug targets? *Br. J. Pharmacol.* **1998**, *125*, 1387−1392.

(3) Hamm, H. E. The Many Faces of G Protein Signali. *J. Biol. Chem.* **1998**, *273*, 669−672.

(4) Civelli, O.; Reinscheid, R. K.; Nothacker, H. P. Orphan receptors, novel neuropeptides and reverse phamaceutical research. *Brain Res.* **1999**, *848*, 63−65.

(5) Hinuma, S.; Habata, Y.; Fujii, R.; Kawamata, Y.; Hosoya, M.; Fukusumi, S.; Kitada, C.; Masuo, Y.; Asano, T.; Matsumoto, H.; Sekiguchi, M.; Kurokawa, T.; Nishimura, O.; Onda, H.; Fujino, M. A prolactin-releasing peptide in the brain. *Nature* **1998**, *393*, 272−302.

(6) Hinuma, S.; Onda, H.; Fujino, M. The quest for novel bioactive peptides utilizing orphan seven-transmembrane-domain receptors. *J. Mol. Med.* **1999**, *77*, 495−504.

(7) Marchese, A.; Heiber, M.; Nguyen, T.; Heng, H. H.; Saldivia, V. R.; Cheng, R.; Murphy, P. M.; Tsui, L. C.; Shi, X.; Gregor, P. Cloning and chromosomal mapping of three novel genes, GPR9, GPR10, and GPR14, encoding receptors related to interleukin 8, neuropeptide Y, and somatostatin receptors. *Genomics* **1995**, *29* (2), 335−344.

(8) Welch, S. K.; O'Hara, B. F.; Kilduff, T. S.; Heller, H. C. Sequence and tissue distribution of a candidate G-coupled receptor cloned from rat hypothalamus. *Biochem. Biophys. Res. Commun.* **1995**, *209* (2), 606−613.

(9) Roland, B. L.; Sutton, S. W.; Wilson, S. J.; Luo, L.; Pyati, J.; Huvar, R.; Erlander, M. G.; Lovenberg, T. W. Anatomical distribution of prolactin-releasing peptide and its receptor suggests additional functions in the central nervous system and periphery. *Endocrinology* **1999**, *140*, 5736−5745.

(10) Ibata, Y.; Iijima, N.; Kataoka, Y.; Kakihara, K.; Tanaka, M.; Hosoya, M.; Hinuma, S. Morphological survey of prolactin-releasing peptide and its receptor with special reference to their functional roles in the brain. *Neurosci. Res.* **2000**, *38* (3), 223−230.

(11) Matsumoto, H.; Maruyama, M.; Noguchi, J.; Horikoshi, Y.; Fujiwara, K.; Kitada, C.; Hinuma, S.; Onda, H.; Nishimura, O.; Inoue, K.; Fujino, M. Stimulation of corticotropin-releasing hormone-mediated adrenocorticotropin secretion by central administration of prolactin-releasing peptide in rats. *Neurosci. Lett.* **2000**, *285* (3), 234−238.

(12) Seal, L. J.; Small, C. J.; Kim, M. S.; Stanley, S. A.; Taheri, S.; Ghatei, M. A.; Bloom, S. R. Prolactin releasing peptide (PrRP) stimulates luteinizing hormone (LH) and follicle stimulating hormone (FSH) via a hypothalamic mechanism in male rats. *Endocrinology* **2000**, *141*, 1909−1912.

(13) Lawrence, C. B.; Celsi, F.; Brennand, J.; Luckman, S. M. Alternative role for prolactin-releasing peptide in the regulation of food intake. *Nat. Neurosci.* **2000**, *7*, 645−646.

(14) Ellacott, K. L.; Lawrence, C. B.; Rothwell, N. J.; Luckman, S. M. PRL-releasing peptide interacts with leptin to reduce food intake and body weight. *Endocrinology* **2002**, *143* (2), 368−374.

(15) Lin, S. H.; Arai, A. C.; Wang, Z.; Nothacker, H. P.; Civelli, O. The Carboxyl Terminus of the Prolactin-Releasing Peptide Receptor Interacts with PDZ Domain Proteins Involved in alpha-Amino-3-hydroxy-5-methylisoxazole-4-propionic Acid Receptor Clustering. *Mol. Pharmacol.* **2001**, *60*, 916−924.

(16) Grundemar, L.; Sheikh, S. P.; Wahlestedt, C. In *Biology of neuropeptide Y and related peptides*; Colmers, W. F., Wahlestedt, C., Eds.; Humana Press: Totowa, NJ, 1993; pp 197−239.

(17) Inui, A. Neuropeptide Y feeding receptors: are multiple subtypes involved? *Trends Pharmacol. Sci.* **1999**, *20*, 43−46.

(18) Darbon, H.; Bernassau, J. M.; Deleuze, C.; Chenu, J.; Roussel, A.; Cambillau, C. Solution conformation of human neuropeptide Y by 1H nuclear magnetic resonance and restrained molecular dynamics. *Eur. J. Biochem.* **1992**, *209* (2), 765−771.

(19) Khiat, A.; Labelle, M.; Boulanger, Y. Three-dimensional structure of the Y1 receptor agonist [Leu31, Pro34]NPY as determinated by NMR and molecular modeling. *J. Pept. Res.* **1998**, *51* (4), 317−322.

(20) Allen, J.; Novotny, J.; Martin, J.; Heinrich, G. Molecular structure of mammalian neuropeptide Y: analysis by molecular cloning and computer-aided comparison with crystal structure of avian homologue. *Proc. Natl. Acad. Sci. U.S.A.* **1987**, *84*, 2532−2536.

(21) Monks, S. A.; Karagianis, G.; Howlett, G. J.; Norton, R. S. Solution structure of human neuropeptide Y. *J. Biomol. NMR* **1996**, *8*, 379−390.

(22) Bader, R.; Bettio, A.; Beck-Sickinger, A. G.; Zerbe, O. Structure and dynamics of micelle-bound neuropeptide Y: comparison with unligated NPY and implications for receptor selection. *J. Mol. Biol.* **2001**, *305*, 307−329.

(23) Douzou, P.; Petsko, G. A. Proteins at work: "Stop-Action" pictures at subzero temperatures. *Adv. Protein Chem.* **1984**, *36*, 245−361.

(24) Fink, A. L. Protein folding in cryosolvents at subzero temperatures. *Methods Enzymol.* **1986**, *131*, 173−187.

(25) Amodeo, P.; Motta, A.; Picone, D.; Saviano, G.; Tancredi, T.; Temussi, P. A. Viscosity as a conformational sieve. NOE of linear peptides in cryoprotective mixtures. *J. Magn. Reson.* **1991**, *95*, 201−207.

(26) Hamada, D.; Kuroda, Y.; Tanaka, T.; Goto, Y. High helical propensity of the peptide fragments derived from beta-lactoglobulin, a predominantly beta-sheet protein. *J. Mol. Biol.* **1995**, *254*, 737−746.

(27) Shiraki, K.; Nishikawa, K.; Goto, Y. Trifluoroethanol-induced stabilization of the alpha-helical structure of beta-lactoglobulin: implication for non-hierarchical protein folding. *J. Mol. Biol.* **1995**, *254*, 180−194.

(28) Sonnichsen, F. D.; Van Eyk, J. E.; Hodges, R. S.; Sykes, B. D. Effect of trifluoroethanol on protein secondary structure: an NMR and CD study using a synthetic actin peptide. *Biochemistry* **1992**, *31*, 8790−8798.

(29) Rajan, R.; Awasthi, S. K.; Bhattachajya, S.; Balaram, P. Teflon-coated peptides: hexafluoroacetone trihydrate as a structure stabilizer for peptides. *Biopolymers* **1997**, *42*, 125−128.

(30) Saviano, G.; Crescenzi, O.; Picone, D.; Temussi, P. A.; Tancredi, T. Solution structure of human β-endorphin in helicogenic solvents: A NMR study. *J. Pept. Sci.* **1999**, *5*, 410−422.

(31) Romano, R.; Dufresne, M.; Prost, M. C.; Bali, J. P.; Bayerl, T. M.; Moroder, L. Peptide Hormone−Membrane Interactions. Intervesicular Transfer of Lipophilic Gastrin Derivative to Artificial Membranes and Their Bioactivities. *Biochim. Biophys. Acta* **1993**, *1145*, 235−242.
(32) Moroder, L.; Romano, R.; Guba, W.; Mierke, D. F.; Kessler, H.; Delporte, C.; Winand, J.; Christophe, J. New Evidence for a Membrane Bound Pathway in Hormone Receptor Binding. *Biochemistry* **1993**, *32*, 13551−13559.
(33) Schwyzer, R. In *Natural Products and Biological Activities*; Imura, H., Goto, T., Murachi, T., Nakajima, T., Eds.; Tokyo Press and Elsevier: Tokyo, 1986; pp 197−207.
(34) Schwyzer, R. Peptide−Membrane Interactions and a New Principle in Quantitative Structure−Activity Realtionships. *Biopolymers* **1991**, *31*, 785−792.
(35) Sargent, D. F.; Schwyzer, R. Membrane Lipid Phase as Catalyst for Peptide−Receptor Interactions. *Proc. Natl. Acad. Sci. U.S.A.* **1986**, *83*, 5774−5778.
(36) Schwyzer, R. Estimated Conformation, Orientation, and Accumulation of Dynorphin A-(1−13)-tridecapeptide on the Surface of Neutral Lipid Membranes. *Biochemistry* **1986**, *25*, 4281−4286.
(37) Schwyzer, R. How Do Peptides Interact with Lipid Membranes and How Does This Affect Their Biological Activity? *Braz. J. Med. Biol. Res.* **1992**, *25*, 1077−1089.
(38) Wüthrich, K. *NMR of Proteins and Nucleic Acids*; John Wiley & Sons: New York, 1986.
(39) Piantini, U.; Soerensen, O. W.; Ernst, R. R. Multiple quantum filters for elucidating NMR coupling networks. *J. Am. Chem. Soc.* **1982**, *104*, 6800−6801.
(40) Bax, A.; Davis, D. G. Mlev-17-based two-dimensional homonuclear magnetization transfer spectroscopy. *J. Magn. Reson.* **1985**, *65*, 355−360.
(41) Jeener, J.; Meyer, B. H.; Bachman, P.; Ernst, R. R. Investigation of exchange processes by two-dimensional NMR spectroscopy. *J. Chem. Phys.* **1979**, *71*, 4546−4553.
(42) Bartels, C.; Xia, T.; Billeter, M.; Guentert, P.; Wüthrich, K. The program XEASY for computer-supported NMR spectral analysis of biological macromolecules. *J. Biomol. NMR* **1995**, *6*, 1−10.
(43) Wishart, D. S.; Sykes, B. D.; Richards, F. M. Relationship between nuclear magnetic resonance chemical shift and protein secondary structure. *J. Mol. Biol.* **1991**, *222*, 311−333.
(44) Wishart, D. S.; Sykes, B. D.; Richards, F. M. The Chemical Shift Index. A Fast and Simple Method for the Assignment of Protein Secondary Structure Trough NMR Spectroscopy. *Biochemistry* **1992**, *31*, 1647−1651.
(45) Dyson, H. J.; Rance, M.; Houghten, R. A.; Wright, P. E.; Lerner, R. A. Folding of immunogenic peptide fragments of proteins in water solution. II. The nascent helix. *J. Mol. Biol.* **1988**, *201*, 201−217.
(46) Guntert, P.; Mumenthaler, C.; Wüthrich, K. Torsion angle dynamics for NMR structure calculation with the new program DYANA. *J. Mol. Biol.* **1997**, *273*, 283−298.
(47) Weiner, S. J.; Kollman, P. A.; Case, D. A.; Singh, U. C.; Chio, C.; Alagona, G.; Profeta, S.; Weiner, P. *J. Am. Chem. Soc.* **1984**, *106*, 765.
(48) Case, D. A.; Pearlman, D. A.; Caldwell, J. W.; Cheatham, T. E., III; Ross, W. S.; Simmerling, C. L.; Darden, T. A.; Merz, K. M.; Stanton, R. V.; Cheng, A. L.; Vincent, J. J.; Crowley, M.; Ferguson, D. M.; Radmer, R. J.; Seibel, G. L.; Singh, U. C.; Weiner, P. K.; Kollman, P. A. *AMBER 5*; University of California, San Francisco: San Francisco, CA, 1997.
(49) Eilers, M.; Shekar, S. C.; Shieh, T.; Smith, S. O.; Fleming, P. J. Internal packing of helical membrane proteins. *Proc. Natl. Acad. Sci.* **2000**, *97*, 5796−5801.
(50) Jarvet, J.; Zdunek, J.; Damberg, P.; Graslund, A. Three-dimensional structure and position of porcine motilin in sodium dodecyl sulfate micelles determined by ^{1}H NMR. *Biochemistry* **1997**, *36* (26), 8153−8163.
(51) Lindberg, M.; Jarvet, J.; Langel, U.; Graslund, A. Secondary structure and position of the cell-penetrating peptide transportan in SDS micelles as determined by NMR. *Biochemistry* **2001**, *40* (10), 3141−3149.
(52) Thompson, J. D.; Higgins, D. G.; Gibson, T. J. CLUSTAL W: improving the sensitivity of progressive multiple sequence alignment through sequence weighting, position-specific gap penalties and weight matrix choice. *Nucleic Acids Res.* **1994**, *22*, 4673−4680.
(53) Cabrele, C.; Beck-Sickinger, A. G. Molecular characterization of the ligand−receptor interaction of the neuropeptide Y family. *J. Pept. Sci.* **2000**, *6* (3), 97−122.
(54) Gill, S. C.; von Hippel, P. H. Calculation of protein extinction coefficients from amino acid sequence data. *Anal. Biochem.* **1989**, *182* (2), 319−326.
(55) Greenfield, N.; Fasman, G. D. Computed circular dichroism spectra for the evaluation of protein conformation. *Biochemistry* **1969**, *8*, 4108−4116.
(56) Lauterwein, J.; Bosch, C.; Brown, L. R.; Wuthrich, K.; Physiochemical studies of the protein−lipid interactions in melittin-containing micelles. *Biochim. Biophys. Acta* **1979**, *556*, 244−264.
(57) MSI Molecular Symulations, 965 Scranton Road, San Diego, CA 92121-3752.

JM020975P